



Fermi National Accelerator Laboratory

FN-382
2521.000
(Submitted to Nucl.
Instrum. Methods)

DESIGN, CONSTRUCTION, AND CALIBRATION OF LARGE ION CHAMBERS FOR MUON FLUX MONITORING IN NEUTRINO BEAMS AT FERMLAB

P. Auchincloss, A. Bodek, R. N. Coleman, H. E. Fisk, C. Haber, T. Kondo,
S. Pordes, P. A. Rapidis, F. Sciulli, M. Shaevitz, E. Villegas, and H. White

March 1983

Design, Construction and Calibration of Large Ion Chambers for
Muon Flux Monitoring in Neutrino Beams at Fermilab

P. Auchincloss^a, A. Bodek^c, R. N. Coleman^b, H. E. Fisk^b,
C. Haber^a, T. Kondo^{b+}, S. Pordes^b, P. A. Rapidis^b,
F. Sciulli^a, M. Shaevitz^a, E. Villegas^b, H. White^b

a. Columbia University, New York, N.Y. 10027

b. Fermi National Accelerator Laboratory,
P.O. Box 500, Batavia, Illinois 60510

c. University of Rochester, Rochester, N.Y. 14627

+. Presently at KEK, 305 Japan

Abstract

This article describes the design, construction, and calibration of three 65" square ion-chambers used to measure the intensity and spatial distribution of the muon flux in the narrow-band neutrino beam at Fermilab. Particular attention has been paid in the design to reducing leakage currents to allow direct calibration of the chambers in a slow-spill beam. As part of the calibration procedure, the change in response due to electromagnetic showers and delta rays accompanying muons as they emerge from material just upstream of the chamber has been measured. The calibration of these ion chambers, which have a total gap of 4 inches, was determined to be 265 ± 5 picocoulombs per 10^6 muons using argon gas at atmospheric pressure.

The problem of measuring the neutrino flux produced by narrow-band secondary beams has been approached in a variety of ways.^{1,2} One of these is to measure both the total secondary beam intensity (with ion-chambers, beam-current transformers, or R.F. cavities) and the particle composition of the beam (i.e. the fractions of pions, kaons and protons) with a Cerenkov counter². These two measurements allow one to infer the absolute number of pions and kaons in the beam, and given their known life-times, branching ratios and decay kinematics to infer the flux of neutrinos. A direct measurement of the flux of muons produced by the pion and kaon decays can provide a powerful crosscheck on the number of pions and kaons derived from the total intensity and particle fraction measurements. The ion-chambers described here were built to measure this flux of muons and determine its spatial distribution at various distances downstream of the secondary beam dump.

Immediately downstream of the secondary beam dump, the muon flux produced by the narrow band beam³ consists of between 10^8 and 10^9 particles largely contained in an area of several square feet; the beam pulse lasts for about a millisecond. Ion-chambers are a natural choice for measuring such fluxes. They have wide dynamic range, are reliable and simple to operate and not subject to gain fluctuations. The wide-dynamic range can be exploited to allow calibration in a slow-spill beam of 10^5 particles per second and to allow operation in a beam of 10^9 per millisecond. This difference of 7 orders of magnitude in instantaneous intensity can be accommodated provided leakage currents are sufficiently small.

Chamber Construction

The chamber construction shown in Figure 1, has been designed with this in mind. The chamber has a total of 5 plates (see figure 2). The chamber walls are made of plexiglas; the internal plates of the chamber sit on machined ceramic spacers which are captured in grooves milled in the plexiglas walls. The two end-panels are of hexcell construction³, 72" square. The outer surface of each end-panel is made of 1/8" thick aluminum; the inner surface of each end-panel is made of 5 machined, printed circuit boards. Each board is 14.2" wide and 6' long, and the printed circuit consists of 10 1.25" wide copper strips separated by 0.15". The strips run horizontally at one end of the chamber and vertically at the other. They run under the plexiglas walls of the chamber to the outside where the electrical connections are made. These strips are used to determine the horizontal and vertical profiles of the muon flux.

The central collecting plate is a 1/8" thick aluminum sheet and the two high-voltage panels are made of hexcell with 1/8" thick aluminum faces. The gap between the central plate and the high-voltage plates is two inches, as is the gap between the profile-plates and their nearest high-voltage plate. The hexcell panels were made in the Neutrino Department Workshop, and are flat to better than +/- 1/64" over their surface. The edges of the panels are sealed with strips of plexiglas to prevent contamination of the chamber by gas from the hexcell paper. By seating the internal plates on ceramic spacers, rather than separating the

plates with continuous frames, the region over which surface leakage currents can flow is reduced from the entire circumference, 260", to a length of 6".

The central collecting plate was further protected against leakage currents by a simple 1/2" wide guard ring made of an insulating layer of Kapton tape attached to the edge of the plate and then covered by a layer of aluminum tape connected to ground potential. Figure 2 shows the electrical connections to the chamber.

Calibration

To obtain a calibration for the chamber, that is the amount of charge collected per muon transversing the chamber, a 2' square chamber was made and exposed to a slow-spill muon "beam". The set-up is shown in Figure 3. (We found it more convenient to make a small chamber than to construct a 6 ft square hodoscope to match a full-size chamber. The small chamber also allowed us to make the tests on the effect of upstream material with a minimum of mechanical difficulty.) The set-up is shown in Figure 3. The muon energy was 200 GeV/c \pm 3% and the flux was concentrated in an area about 6" square with a halo of about 5% the central intensity extending at least 1' horizontally. The counters A,B,C and D were cut to match the size of the central plate of the ion-chamber and carefully aligned with respect to each other. The light-guides and photomultiplier tubes were mounted on successive edges of the

counters to avoid coincidences from muons producing Cerenkov light in the material of the light-guides.

The calibration electronics consisted of a set of discriminators, coincidence and scaler modules to measure the rates of each counter, the four-fold coincidence and all three-fold coincidences, plus a charge integrator⁵ to measure the charge from the ion-chamber. The integrator uses a Teledyne Philbrick 1702 parametric amplifier which has an input bias current of less than 5 femtoamps, and bandwidth of 100 hz - which is quite acceptable in a slow-spill beam. The output of the charge integrator was fed to an Analog to Digital (A to D) converter. The data written to tape each beam spill included all individual counter rates and coincidences plus eighty samples of the A to D output taken over a period starting one second before the beam spill and finishing a second after the spill. The typical spill lasted .800 milliseconds and contained 120000 muons. Figure 4 shows the output voltage of the integrator for a typical cycle. The integrator itself has been calibrated to better than 2% with a precision Pico-Ampere Source⁶. The A to D converter has been calibrated to 0.1% with a precision voltage source.

The chamber was run on Argon gas at atmospheric pressure. At these low intensities, the plateau was reached with 150 volts across the gap. The chamber did not break-down nor exhibit any significant leakage current up to 5000 volts, and we ran at 500 volts. (It should be noted that when operating in the vastly more intense flux

of muons produced by the narrow-band beam, the chambers only reached plateau at 2200 volts).

Four sets of data were taken:

1. With no extra material upstream of the chamber
2. With a 2 1/2" thick iron plate just in front of the chamber
3. With 5" of iron just in front of the chamber.
4. With 1" of plastic just in front of the chamber.

In configuration 1, the nearest material was the steel muon filter some 30 feet upstream. The data were analyzed, pulse by pulse, by fitting straight-lines to the integrator output samples taken before and after the spill and calculating the voltage difference, DV, between these fits at the midpoint of the spill. In principle, the slopes of the lines before and after the spill, which depend on the drift of the integrator, could be significantly different, particularly given the large variations in line-voltage during the accelerator cycle. In practice, the slopes were sufficiently similar to make the results insensitive to where during the spill DV was calculated. The output of the integrator on accelerator cycles where no beam was extracted (but the line-voltage went through its usual contortions) showed no unusual behavior during the spill-time, so we believe our extrapolation procedure introduces no systematic error. The voltage difference, DV, is converted to obtain the charge collected, Q, by the relation $Q = DV \times 10.2$ picocoulombs.

For convenience, we define the calibration constant in units of pico-coulombs/ 10^6 muons. The scintillation counters A,B,C and D had an average efficiency of 98%, and a correction of +0.5% is made to obtain the true flux from the > 3 out of 4 coincidence. Corrections due to two muons in the same accelerator R.F. bucket - which register as a single count in the scintillation counters - are + 1/2% for most intensities⁷. To compensate for any intensity dependent inefficiencies in the counters, the effective calibration constant is plotted as a function of the beam intensity for each data set. Figure 5 shows such a plot for data set (1). (The error-bars correspond to the r.m.s. of the constants derived from different beam-pulses at each intensity.) This data shows essentially no dependence on beam-intensity. The data taken with material in front of the chamber, however, all show some intensity dependence. We believe that this is due to the poor spill structure at high intensities which increases the correction required for more than one particle in the same R.F. bucket.

The calibration constants for the different data sets are given in Table 1. The values given are those obtained at intensities below 120000 particles per spill; to allow for the observed intensity dependence, the error given is the sum of the r.m.s error on the value quoted plus half the difference between this value and the intercept at zero intensity of a straight-line fit to the calibration constant vs intensity. We should note that in operation (i.e. when exposed to the muon flux from the dichromatic neutrino beam) the chambers response was linear with incident flux (as determined by monitoring devices upstream) to better than 2%.

We use the difference between "no material" and "1 of plastic" to estimate the contribution to the measured charge from delta-rays produced in the upstream-counters. In fact, since the extra material was closer to the chamber than the upstream counters, its contribution sets an upper limit to the effect of the counters themselves. The effect of the material was to increase the calibration constant by 2.6%; we have taken the effect of the counters as 1.5% +/- 1.5%. Subtracting this contribution from the "no material" value, gives an effective calibration constant of 265 +/- 4 pc/10⁶ muons. It is instructive to compare this with the calibration constant expected for 4" of Argon gas as follows. A 200 GeV muon loses energy at a rate 1.45 times minimum ionizing, and deposits 35.4 KeV in the gas at 20°C and atmospheric pressure. The average energy needed to make an ion pair in Argon is 26 eV⁸, implying that 1360 ion pairs are produced per muon and giving a calibration constant of 218 pc/10⁶ muons. We attribute the 20% difference between our measured calibration and the calculated value to ionization produced by electrons knocked out of the upstream chamber plates. It should be noted that a similar comparison between calculated and measured calibration constants for the thin-plate (0.002" aluminum) ion-chambers used to determine the secondary hadron beam flux shows a much larger discrepancy; in that case, there is a considerable contribution to the ionization from slow nuclear fragments produced in inelastic collisions of the beam and the chamber plates.^{2,9}

Influence of Material Upstream

We show the fractional change in chamber response versus the amount of material immediately upstream of the chamber in Figure 6. These measurements are of interest for two main reasons. The first is that some of the monitoring ports in the muon shield are narrow so that the ion-chambers will be close to the upstream-wall¹⁰; the intensities recorded by these chambers will need to be corrected for the ionizing radiation (electrons and photons) accompanying the muon flux from muon interactions in the walls. A second is to compare our results with the experience at CERN where the muon flux is monitored by solid-state detectors (SSD's) placed in narrow ports in the muon shield. The corrections for ionization from the products of muon interactions in the walls have been determined in a completely different way¹¹, by exposing emulsions in the muon-shield and counting the relative numbers of muons and delta-rays (wide-angle tracks). Some 25% of the signal recorded by these SSD's is attributed to delta-rays. Comparing this result to Fig. 6, the CERN result and our measurement are in rough agreement.

Operating Experience

It should be noted, as emphasized in reference 11a, that delta-rays not only contribute to the total intensity recorded by the ion-chamber, but also tend to smear the intensity profiles since they emerge at large angles. Two of the chambers described here were used during the narrow-band neutrino running in spring 1982.

To avoid both the above problems, they were installed some tens of ft downstream of the secondary beam dump, with essentially no material (except air) between the dump and the chambers. The charge collected by the total intensity plate was measured with a Fermilab-designed high rate charge-digitizer¹², and the charge collected on each of the strips on the end-plates was measured with the standard beam-line SWIC scanner¹³. As a basic check of the reproducibility of the chamber response, the two chambers were placed with one immediately in front of the other 68ft downstream of the dump. Pulse by pulse the chambers gave the same response within 3%. For the rest of the running, the chambers were separated with the upstream chamber placed 17' from the dump and the downstream chamber 97' from the dump. (Figure 7 shows the location of the chambers along the neutrino beam-line.)

Figure 8 shows the linearity of the chamber response in-place; the horizontal axis is the secondary beam intensity as measured by an ion-chamber in the secondary beam. Figures 9a and 9b show horizontal and vertical profiles, obtained when the secondary momentum was set for 100 GeV/c and 200 GeV/c positive particles respectively. Most of the muons come from pion decays all of whose decay muons pass through the chamber. The offset of the horizontal profile is due to the architecture of the beam-dump enclosure, which does not provide room to center the chamber on the neutrino beam. Figure 10 shows the profile obtained when a 200 GeV primary proton beam was transported to the secondary dump. (This background of muons produced in the dump has to be measured and subtracted from

the observed flux to determine the muon flux from pion and kaon decay before the dump). Preliminary analysis of the data obtained shows agreement between the observed muon flux and the muon flux predicted from the measurements of the secondary beam within 10%.

Acknowledgements

We thank the personnel of the Neutrino Department and particularly, A. Raymond and Vivian Jacobsen , for their careful work in the construction of these devices. We also thank the members of E-673 (spokesperson J. Cooper) for all their help with the N-1 beam line.

References

1. G. Cavallari et al., IEEE, Vol NS-25, No.1, (1978), 600
J.G.H. de Groot et al., Z. Phys(1(1979) 143
2. A. Bodek et al., UR837 (1983) to be published in Z. Phys.
C.

R. Blair, Thesis, (Unpublished) California Inst. of
Technology, 1982.
3. A. Bodek et al., to be published in

R. Blair, Thesis, (Unpublished) California Inst. of
Technology, 1982.
4. D. Edwards and F. Sciulli, Fermilab TM 660
5. Verticel Honeycomb, Melrose Park, Illinois
3M Scotch-Weld Structural Adhesive 2158A & B
6. Designed by O. Fackler, Rockefeller University, New York
7. Keithley Model 261 Pico-amp Source
8. The spill was monitored by E-673 who were the primary users
of the N-1 Line
9. Table 1 of F. Sauli, Principles of Operations of Multiwire
Proportional and Drift Chambers CERN 77-09
10. M.V. Purohit, Ion Chamber Calibration, E-616 internal
memorandum
11. J. Peoples and D. Theriot, Fermilab TM 950
12. E. Heijne, CERN/EF/Beam 79-4
H. Burmeister et al., CERN/EP/NBO 79-9
13. A. R. Donaldson, High-Rate Charge Digitizer, IEEE
NS-26, (1979), 3439

14. W. Higgins, Swic-Scanner Manual, Fermilab TM 868 (1979)

Table 1

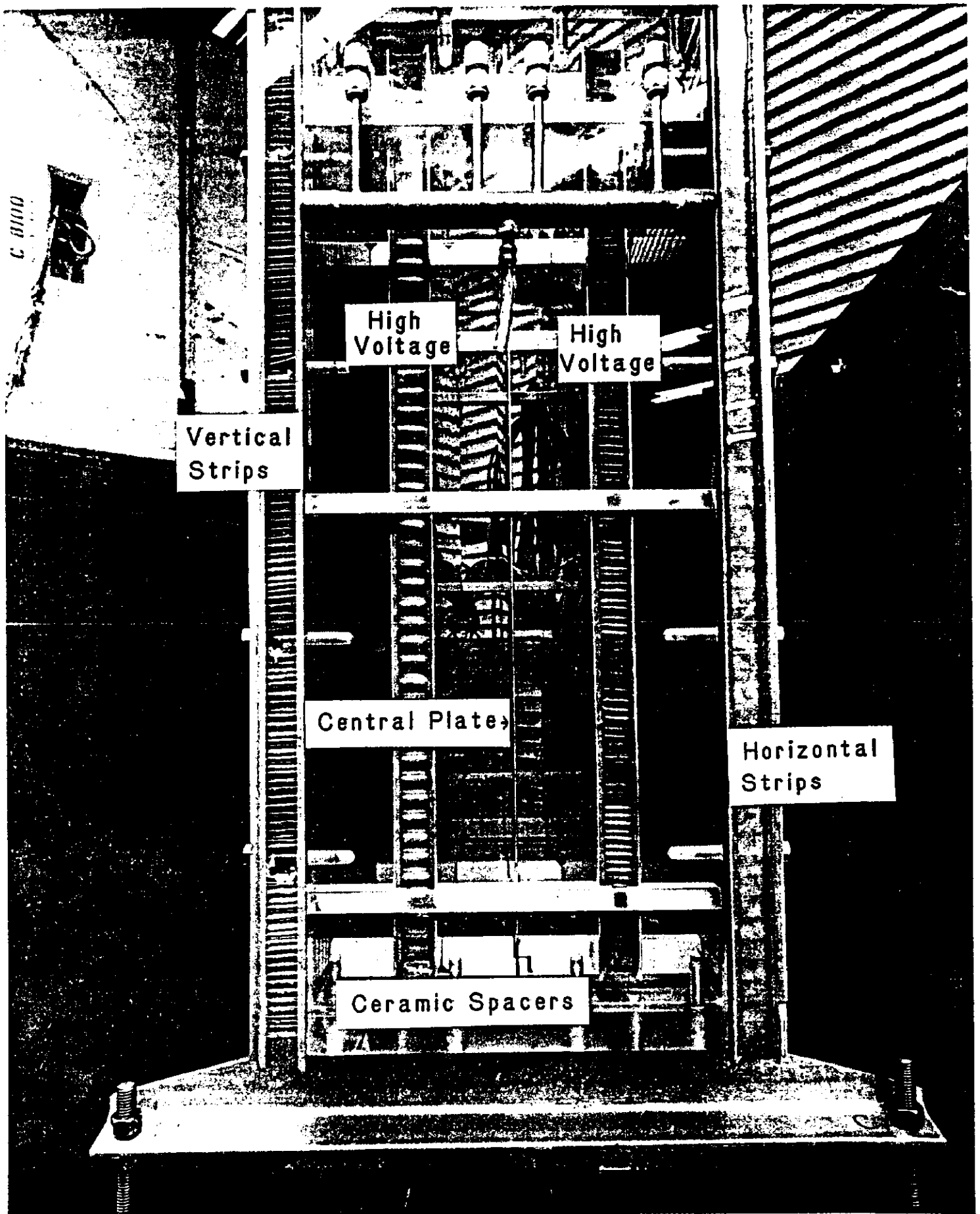
Condition:	Calibration Constant (pC/10 ⁶ muons)
No Extra Material:	270 ± 4
2 1/2" of Iron	340 ± 10
5" of Iron	365 ± 15
1" of Plastic	277 ± 4

Figure Captions

1. A view of the small Chamber from the side
2. Electrical Connections to chamber
3. Calibration Set-up
4. Output of Charge Integrator on Typical Cycle
5. Calibration constant versus intensity, data set(1)
6. Change in calibration versus amount of material upstream of the ion-chamber.
7. Arrangement of Muon Chambers along the Neutrino Beam
8. Linearity plot of chamber response in place
9. Muon flux profiles from neutrino beams at +100

10. Muon flux profile from proton interactions in the secondary beam dump. About 5% of the flux seen in figures 9a and 9b comes from these interactions in the secondary beam dump.

Figure 1



ELECTRICAL CONNECTIONS

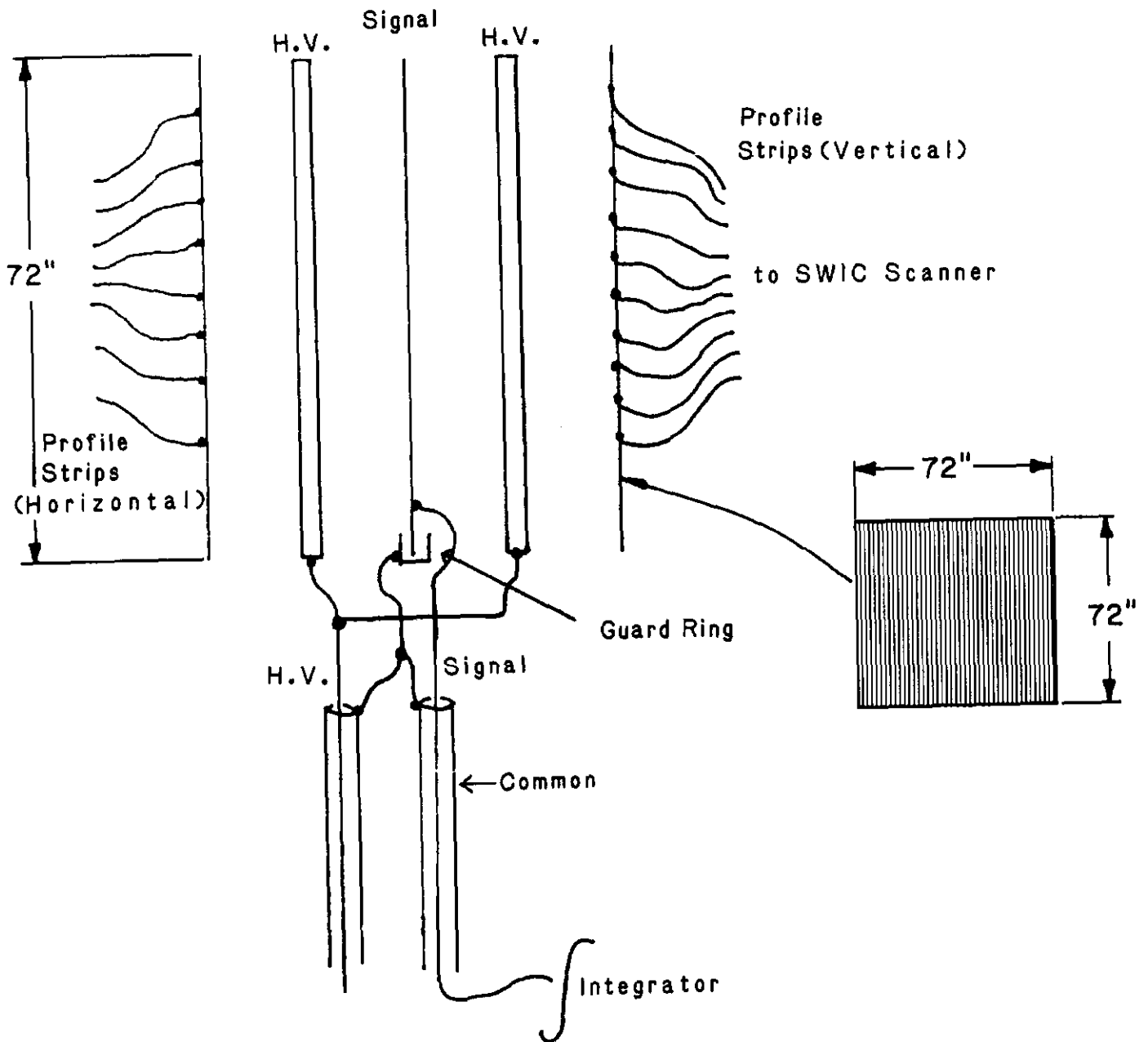


Fig. 2

CALIBRATION SET-UP

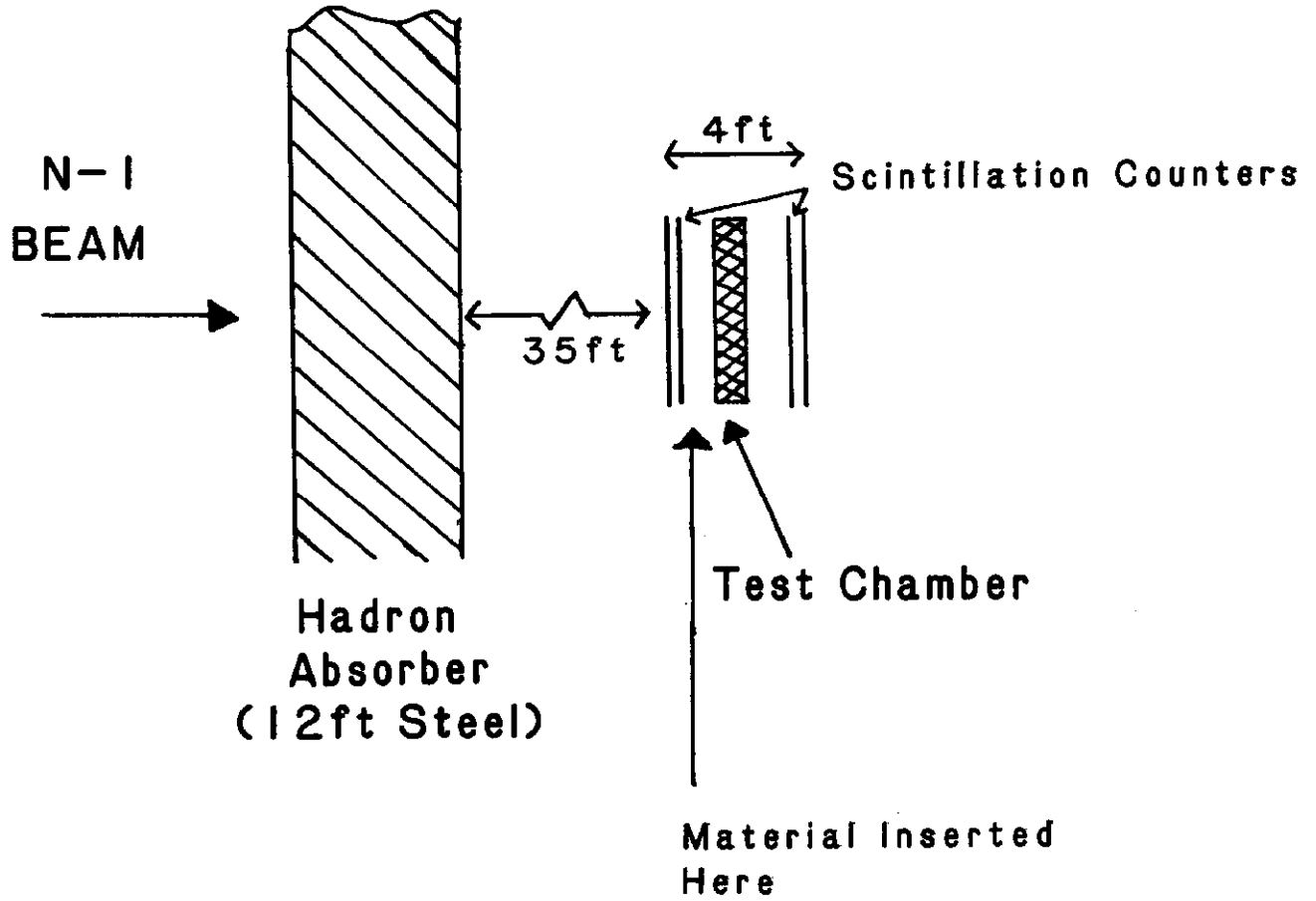


Fig. 3

Integrator Output

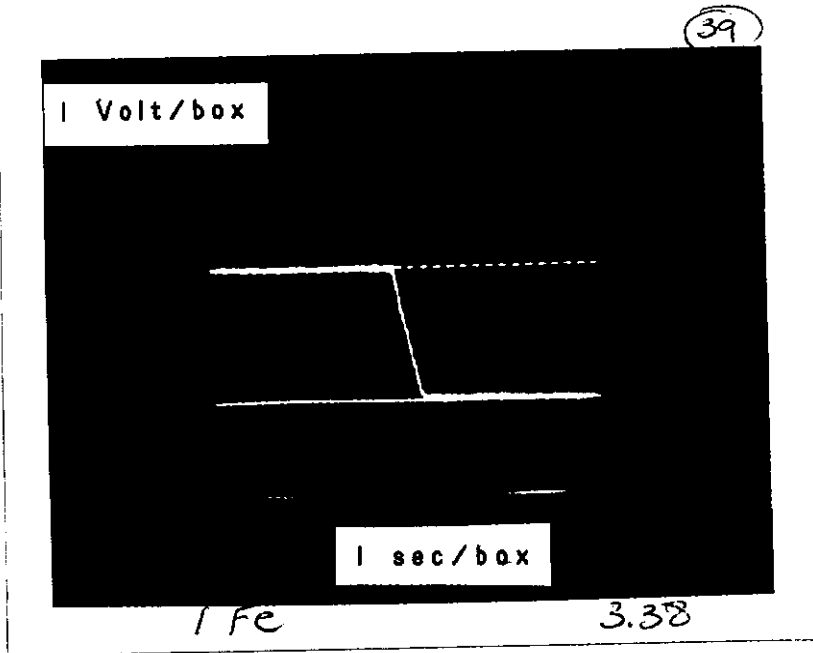


Fig. 4

CALIBRATION CONSTANT vs. SPILL INTENSITY

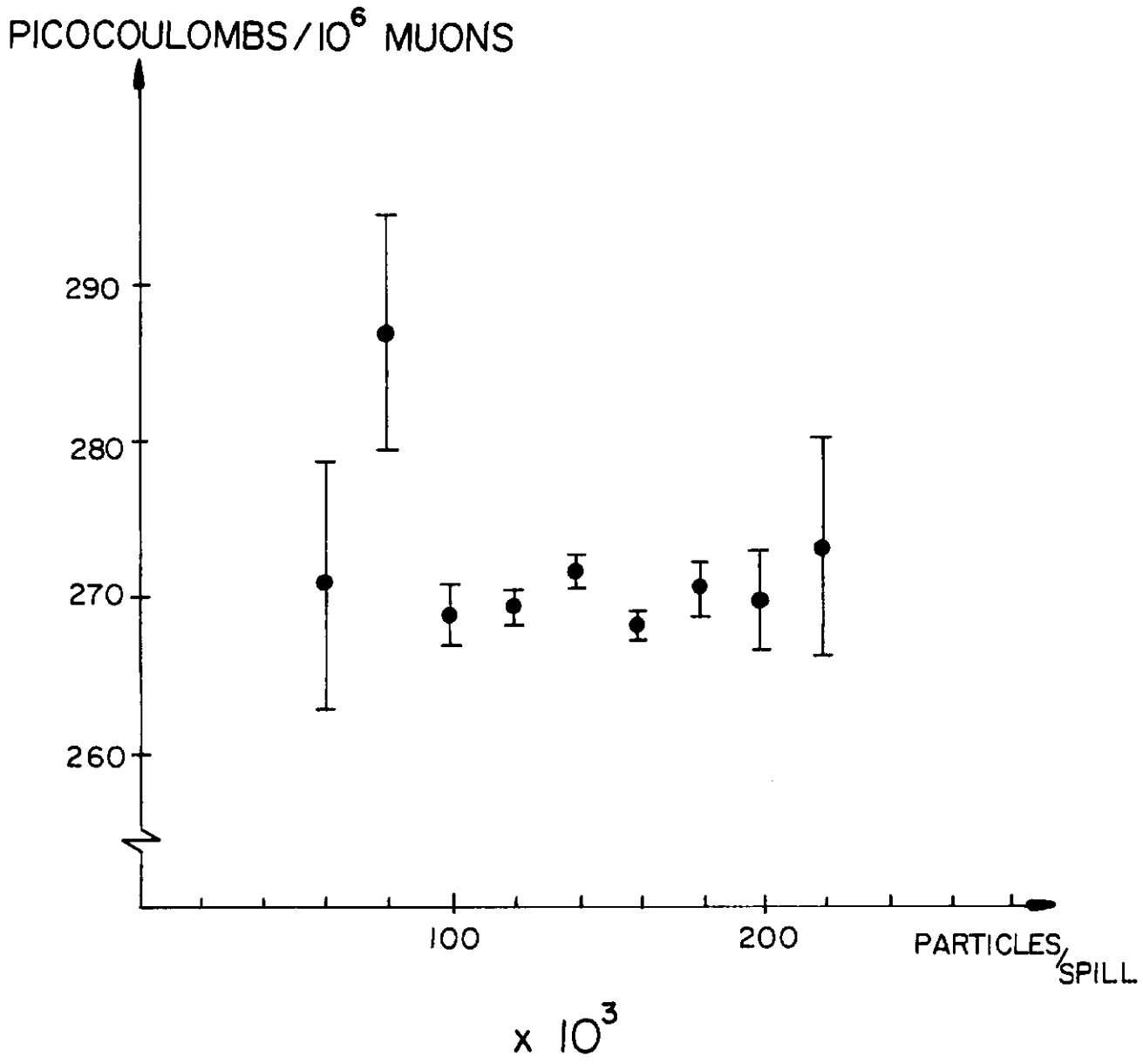


Fig. 5

% INCREASE IN SIGNAL
vs. AMOUNT OF MATERIAL

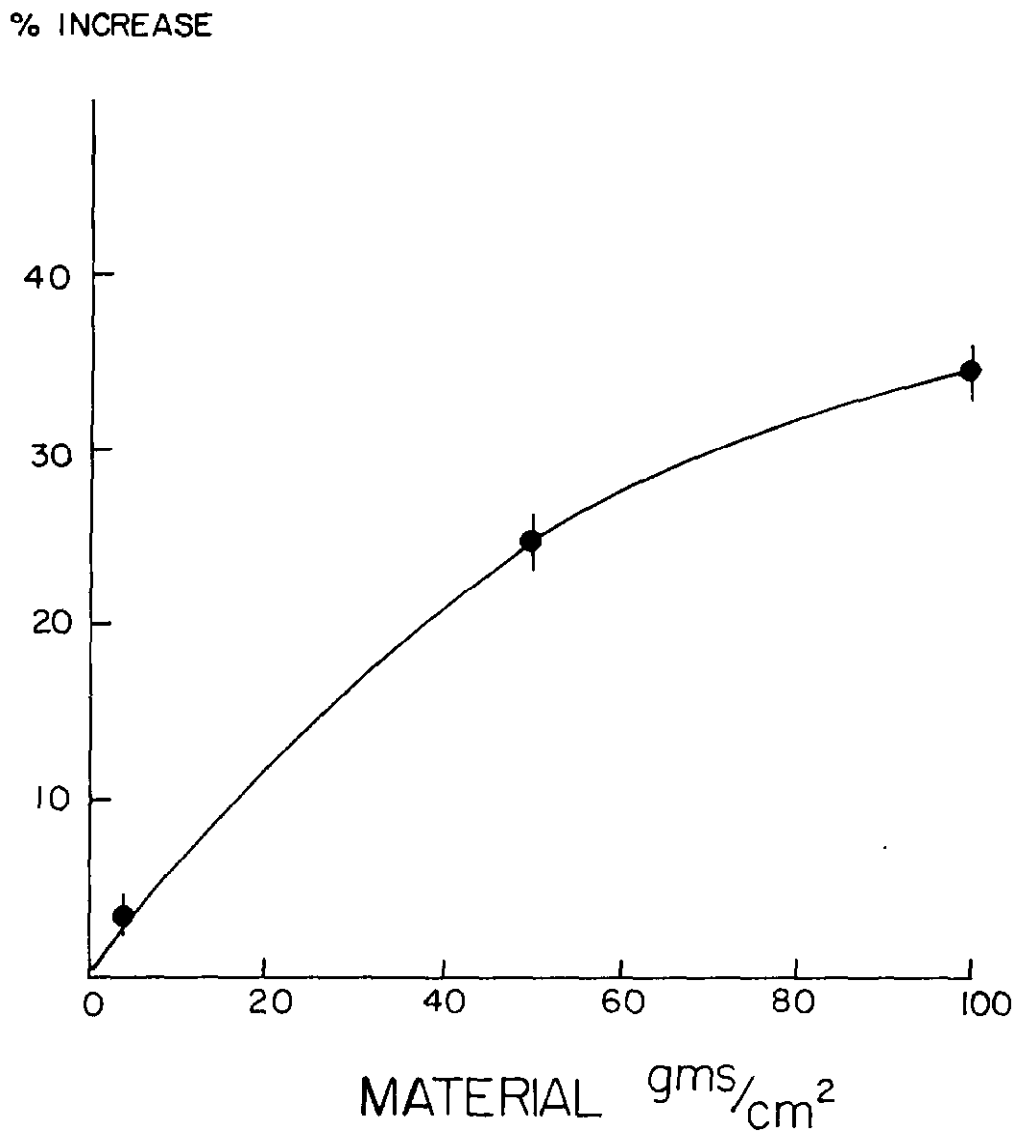


Fig. 6

LAYOUT OF NEUTRINO LINE
SHOWING POSITION OF MUON FLUX MONITORS
(NOT TO ANY SCALE)

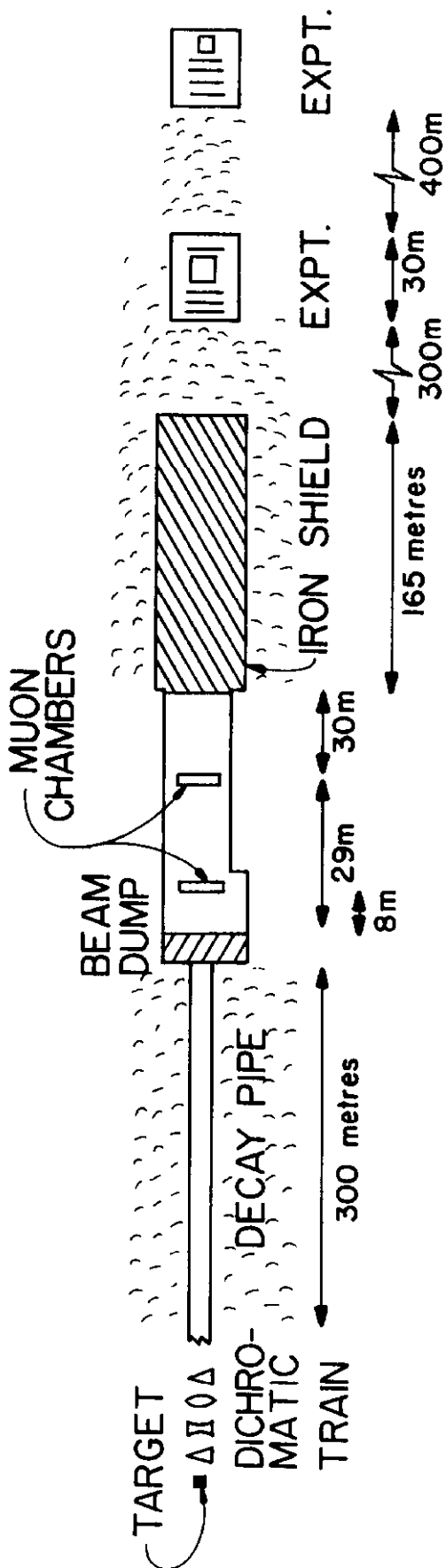


Fig. 7

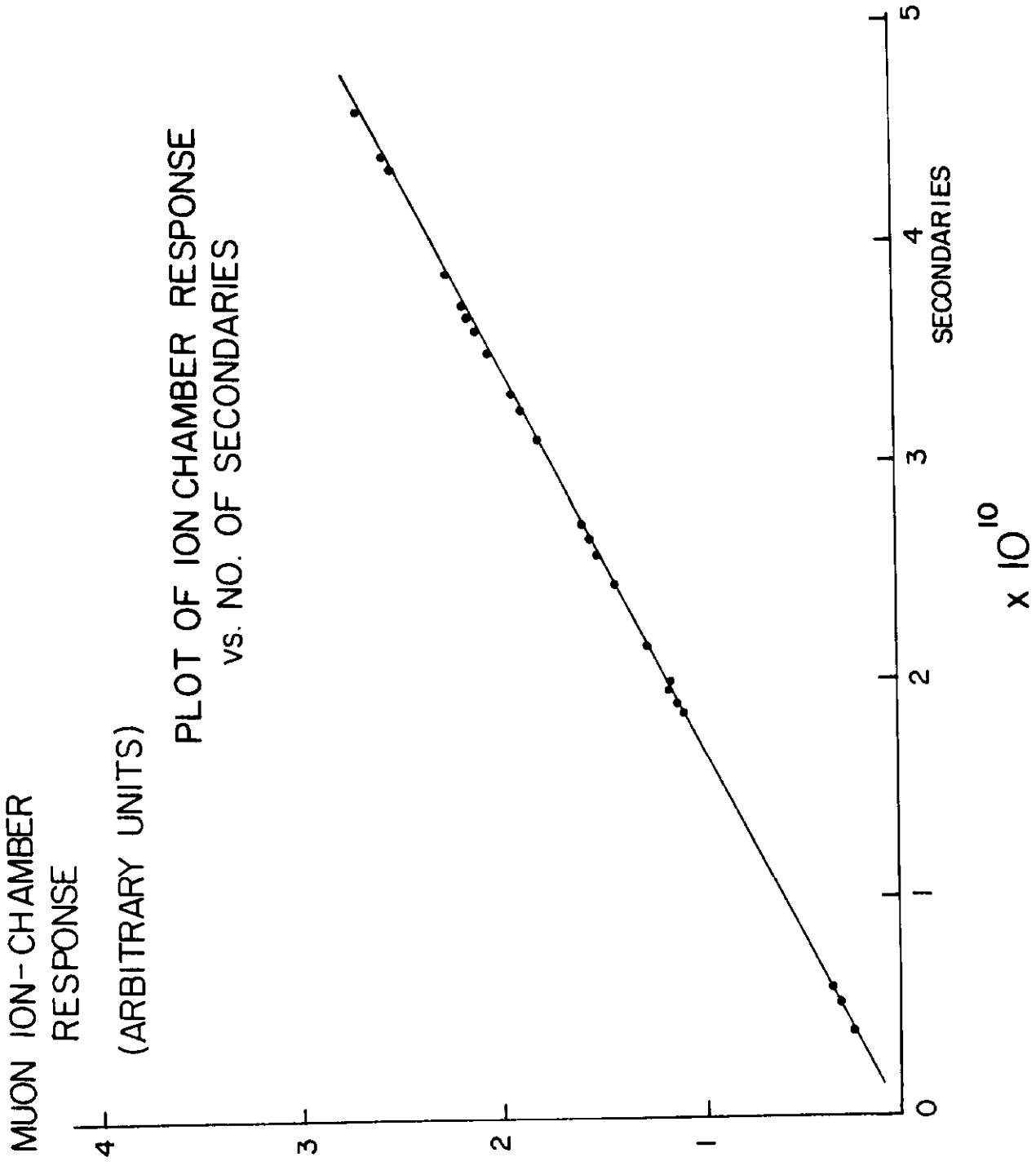


Fig. 8

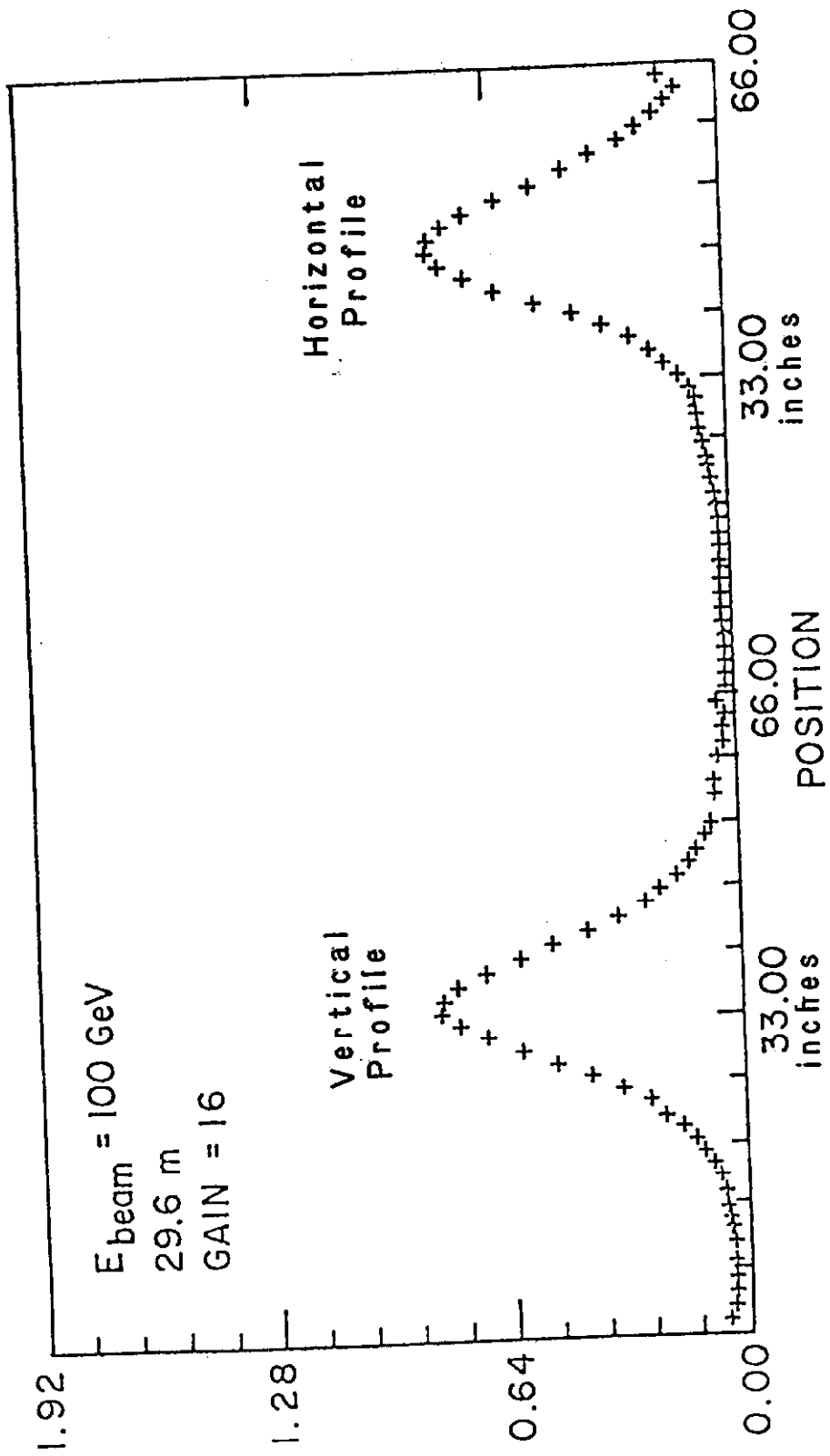


Fig. 9a

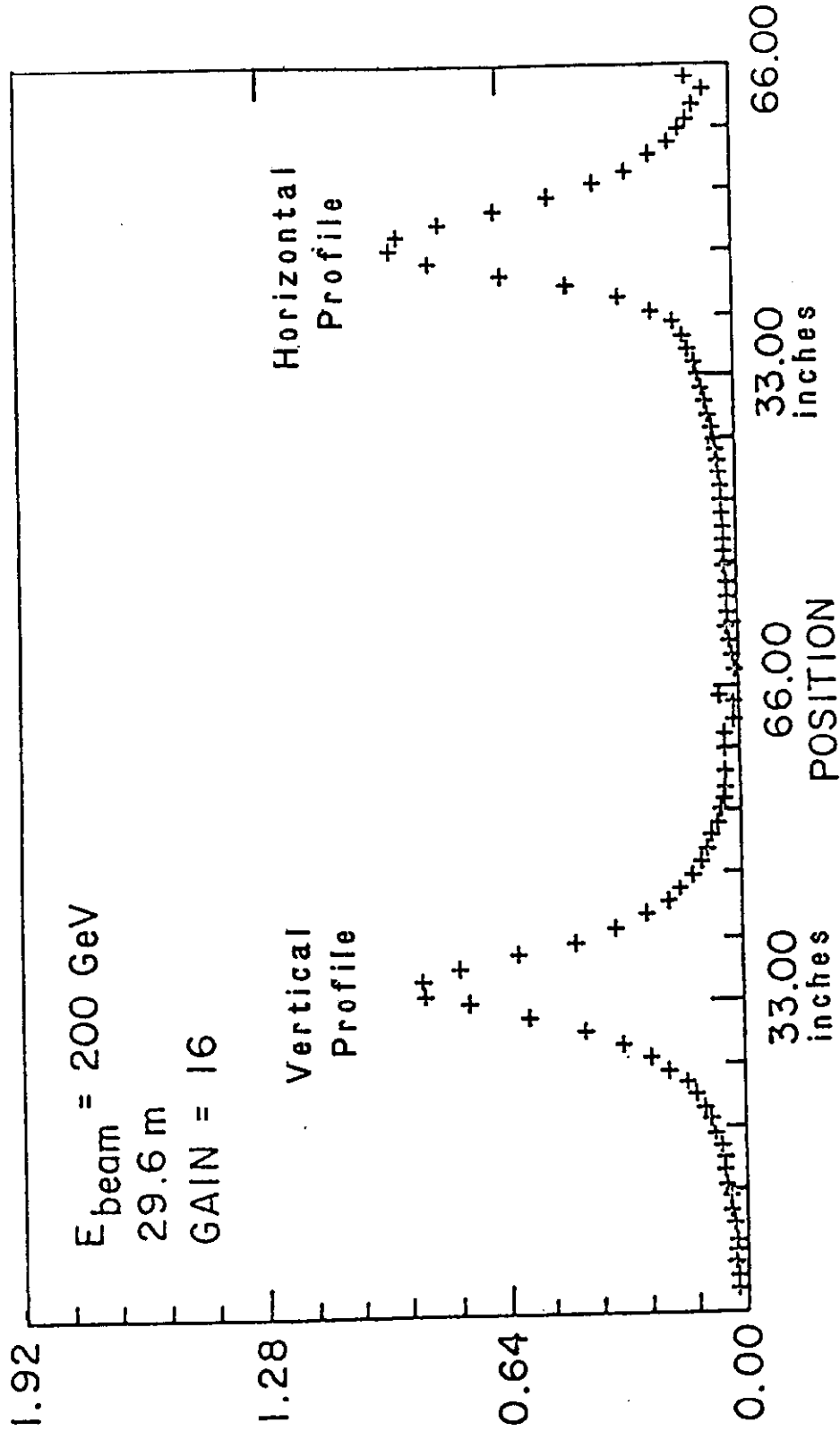


Fig. 9b

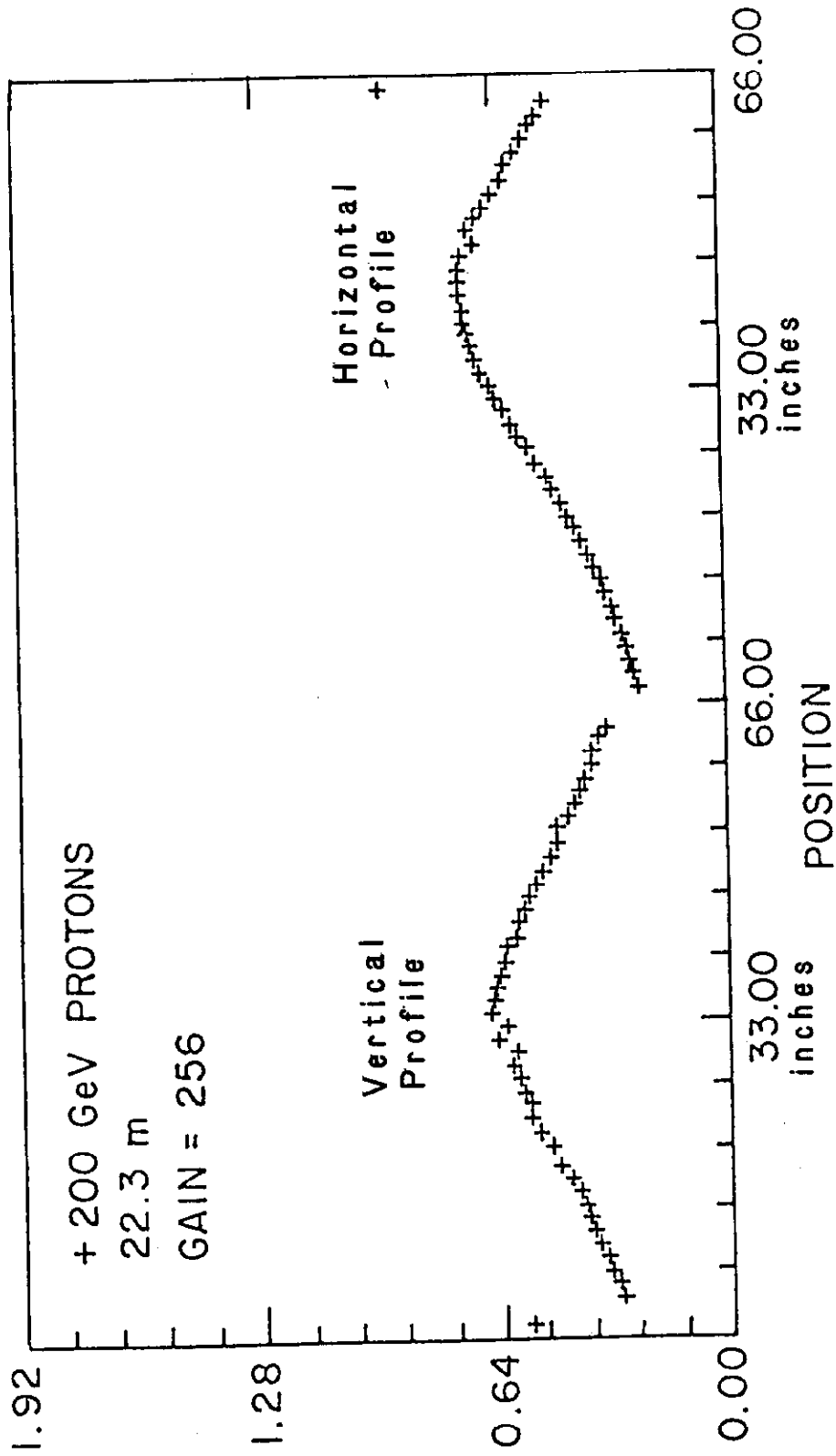


Fig. 10